High-Order Finite Element for the resolution of time-harmonic Maxwell equations

G. Cohen, M. Duruflé

INRIA Rocquencourt

Outline of the presentation

- Analysis of quadrilateral finite element with eigenvalue computations.
  Edge finite element and Discontinuous Galerkin method.

Outline of the presentation

- Analysis of quadrilateral finite element with eigenvalue computations.
  Edge finite element and Discontinuous Galerkin method.

- Convergence of these methods for the scattering of a disk.

Outline of the presentation

- Analysis of quadrilateral finite element with eigenvalue computations.
  Edge finite element and Discontinuous Galerkin method.
- Convergence of these methods for the scattering of a disk.
- Comparative study with triangles for the scattering of a diedron-disk.

Outline of the presentation

- Analysis of quadrilateral finite element with eigenvalue computations.
  Edge finite element and Discontinuous Galerkin method.
- Convergence of these methods for the scattering of a disk.
- Comparative study with triangles for the scattering of a diedron-disk.
- Numerical results in 3-D

Eigenvalue Problem

Find $(\omega, \vec{E}, \vec{H}) \neq (0,0,0)$ so that

$$
\begin{aligned}
-i\omega \;\; \varepsilon(x)\, \vec{E}(x) \; - \; \text{curl}\, \vec{H}(x) &= 0 \quad x \in \Omega \\
-i\omega \;\; \mu(x)\, \vec{H}(x) \; + \; \text{curl}\, \vec{E}(x) &= 0 \quad x \in \Omega \\
\nu \times \vec{E}(x) &= 0 \quad x \in \Gamma
\end{aligned}
\tag{1}
$$

Eigenvalue Problem

Find $(\omega, \vec{E}, \vec{H}) \neq (0,0,0)$ so that

$$\begin{aligned}
-i\omega\ \varepsilon(x)\,\vec{E}(x)\ -\ \text{curl}\,\vec{H}(x) &= 0 \quad x \in \Omega \\
-i\omega\ \mu(x)\,\vec{H}(x)\ +\ \text{curl}\,\vec{E}(x) &= 0 \quad x \in \Omega \\
\nu \times \vec{E}(x) &= 0 \quad x \in \Gamma
\end{aligned} \tag{1}$$

Use of second order formulation :

$$-\omega^2 \vec{E}(x)\ +\ \text{curl}\left(\frac{1}{\mu(x)}\text{curl}(\vec{E}(x))\right)\ =\ 0$$

A first approach : discretization of the H(curl) space

Variational formulation of second order in $\vec{E}$

$$-k^2 \int_\Omega \varepsilon_r \, \vec{E} \cdot \vec{\varphi} + \int_\Omega \frac{1}{\mu_r} (\nabla \times \vec{E}) \cdot (\nabla \times \vec{\varphi}) = 0 \qquad (2)$$

A first approach : discretization of the H(curl) space

Variational formulation of second order in $\vec{E}$

$$-k^2 \int_\Omega \varepsilon_r \, \vec{E} \cdot \vec{\varphi} + \int_\Omega \frac{1}{\mu_r} (\nabla \times \vec{E}) \cdot (\nabla \times \vec{\varphi}) = 0 \tag{2}$$

$$\vec{E}, \vec{\varphi} \in \text{H(curl,}\Omega\text{)} = \{\vec{u} \in \left(L^2(\Omega) \right)^2 \text{ and } \nabla \times \vec{u} \in L^2(\Omega)\}$$

A first approach : discretization of the H(curl) space

Variational formulation of second order in $\vec{E}$

$$-k^2 \int_\Omega \varepsilon_r \, \vec{E} \cdot \vec{\varphi} + \int_\Omega \frac{1}{\mu_r} (\nabla \times \vec{E}) \cdot (\nabla \times \vec{\varphi}) = 0 \qquad (2)$$

$$\vec{E}, \vec{\varphi} \in \text{H(curl,}\Omega) = \{\vec{u} \in \left(L^2(\Omega)\right)^2 \text{ and } \nabla \times \vec{u} \in L^2(\Omega)\}$$

After discretization, we obtain the eigenvalue system :

$$-\omega^2 M_h E - K_h E = 0$$

A first approach : discretization of the H(curl) space

Variational formulation of second order in $\vec{E}$

$$-k^2 \int_\Omega \varepsilon_r \, \vec{E} \cdot \vec{\varphi} + \int_\Omega \frac{1}{\mu_r} (\nabla \times \vec{E}) \cdot (\nabla \times \vec{\varphi}) = 0 \qquad (2)$$

$$\vec{E}, \vec{\varphi} \in \text{H(curl},\Omega) = \{\vec{u} \in \left(L^2(\Omega) \right)^2 \text{ and } \nabla \times \vec{u} \in L^2(\Omega)\}$$

After discretization, we obtain the eigenvalue system :

$$-\omega^2 M_h E - K_h E = 0$$

Use of Arpack++ to solve this eigenvalue system

Nedelec's first family on quadrilaterals

Space of approximation

$$V_h = \{ \vec{u} \in \text{H(curl,}\Omega\text{) so that } DF_i^t \, \vec{u} \circ F_i \in Q_{r-1,r} \times Q_{r,r-1} \} \qquad (3)$$

Nedelec's first family on quadrilaterals

Space of approximation

$$V_h \; = \; \{ \, \vec{u} \in \; \text{H(curl,}\Omega) \; \text{ so that } DF_i^t \, \vec{u} \circ F_i \; \in Q_{r-1,r} \; \times \; Q_{r,r-1} \, \} \qquad (3)$$

Basis functions

$$\begin{aligned} \vec{\hat{\varphi}}^1_{i,j}(\hat{x}, \hat{y}) \;&=\; \hat{\psi}_i^G(\hat{x}) \, \hat{\psi}_j^{GL}(\hat{y}) \, \vec{e_x} \quad 1 \leq i \leq r \quad 1 \leq j \leq r+1 \\ \vec{\hat{\varphi}}^2_{j,i}(\hat{x}, \hat{y}) \;&=\; \hat{\psi}_j^{GL}(\hat{x}) \, \hat{\psi}_i^G(\hat{y}) \, \vec{e_y} \quad 1 \leq i \leq r \quad 1 \leq j \leq r+1 \end{aligned} \qquad (3)$$

Nedelec's first family on quadrilaterals

Space of approximation

$$V_h = \{ \vec{u} \in \text{ H(curl,}\Omega\text{) so that } DF_i^t \, \vec{u} \circ F_i \in Q_{r-1,r} \times Q_{r,r-1} \} \qquad (3)$$

Basis functions

$$\begin{aligned} \vec{\hat{\varphi}}^1_{i,j}(\hat{x},\hat{y}) &= \hat{\psi}_i^G(\hat{x}) \, \hat{\psi}_j^{GL}(\hat{y}) \, \vec{e_x} \quad 1 \leq i \leq r \quad 1 \leq j \leq r+1 \\ \vec{\hat{\varphi}}^2_{j,i}(\hat{x},\hat{y}) &= \hat{\psi}_j^{GL}(\hat{x}) \, \hat{\psi}_i^G(\hat{y}) \, \vec{e_y} \quad 1 \leq i \leq r \quad 1 \leq j \leq r+1 \end{aligned} \qquad (3)$$

ψ_i^G, ψ_i^{GL} lagrangian functions linked with respectively Gauss and Gauss-Lobatto points.

Eigenmodes with the first family

Mesh used for the simulations (Q5)

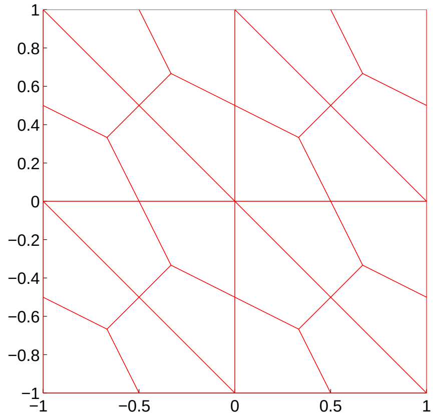

Eigenmodes with the first family

$\omega^2 = 32.076$

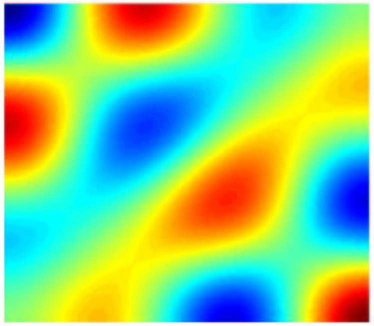

$\omega^2 = 32.076$

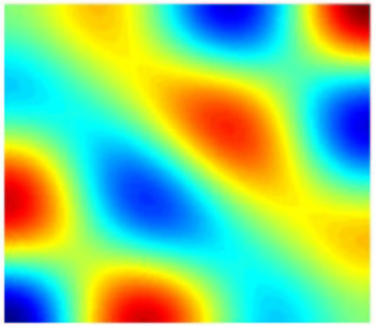

$\omega^2 = 39.478$

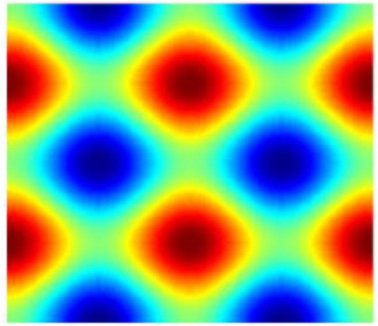

Eigenmodes with the first family

$\omega^2 = 32.076$ $\omega^2 = 32.076$ $\omega^2 = 39.478$

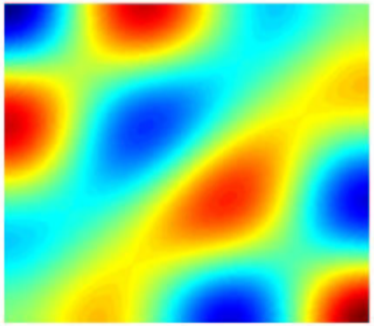
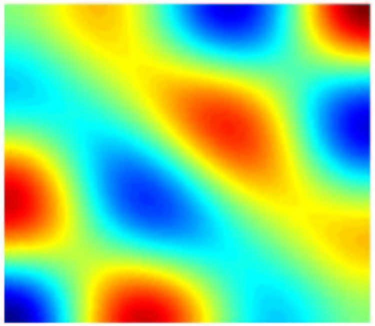
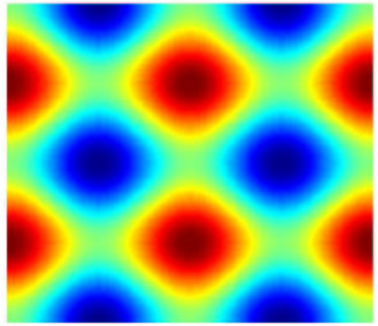

$\omega^2 = 32.076$ $\omega^2 = 41.945$ $\omega^2 = 41.945$

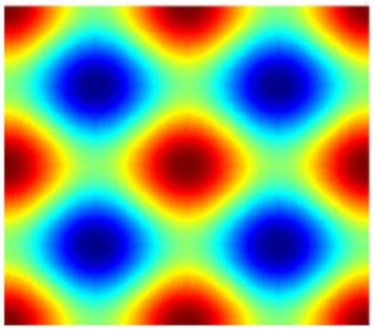
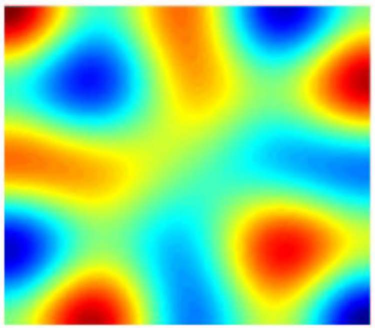
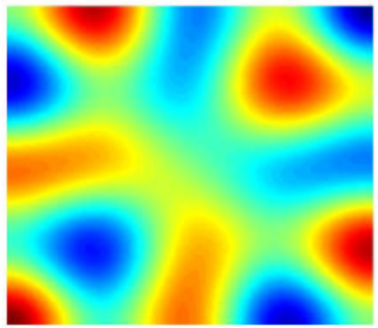

- Nedelec's first family seems spectrally correct on quadrilaterals and triangles.

Nedelec's second family for quadrilaterals

Space of approximation

$$V_h = \{ \vec{u} \in \text{ H(curl,}\Omega\text{) such as } DF_i^t \, \vec{u} \circ F_i \in (Q_r)^2 \} \quad (4)$$

Nedelec's second family for quadrilaterals

Space of approximation

$$V_h \;=\; \{\, \vec{u} \in \; \text{H(curl,}\Omega\text{) such as } DF_i^t\, \vec{u} \circ F_i \;\in (Q_r)^2 \,\} \qquad (4)$$

Use of Gauss-Lobatto points both for integration and interpolation

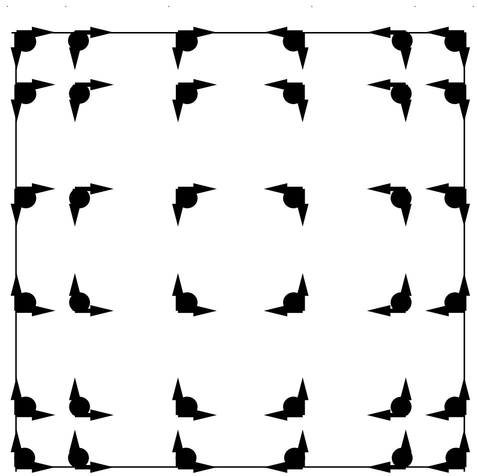

Nedelec's second family for quadrilaterals

Space of approximation

$$V_h \;=\; \{\, \vec{u} \in \text{ H(curl,}\Omega\text{) such as } DF_i^t\, \vec{u} \circ F_i \,\in (Q_r)^2 \,\} \qquad (4)$$

Use of Gauss-Lobatto points both for integration and interpolation

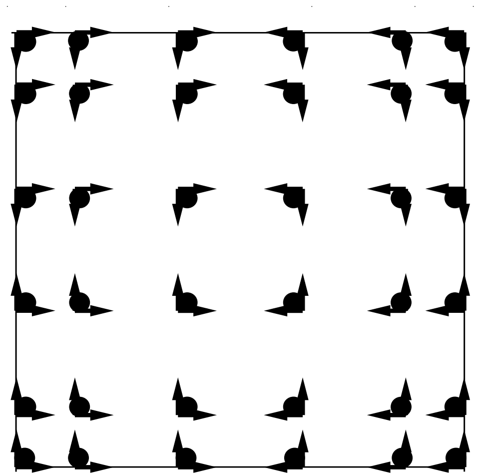

- Mass matrix block-diagonal (mass-lumping)
- Gain in storage and time for the matrix-vector product

Eigenmodes with the second family

Mesh used for the simulations (Q5)

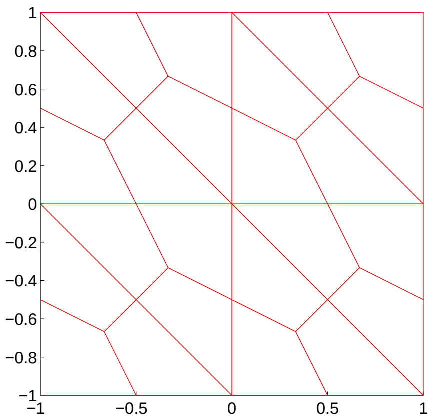

Eigenmodes with the second family

$\omega^2 = 32.08$ $\omega^2 = 32.08$ $\omega^2 = 37.54$ $\omega^2 = 37.95$

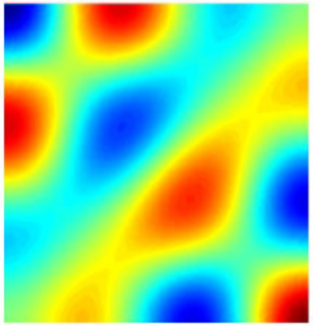

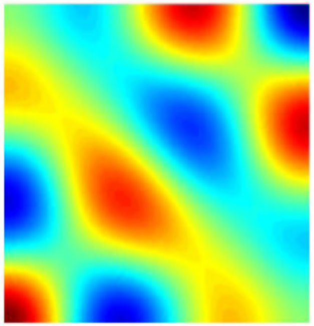

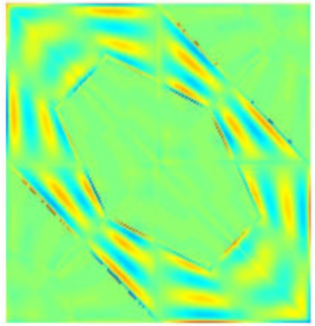

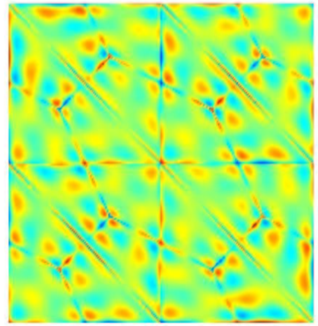

Eigenmodes with the second family

$\omega^2 = 32.08$ $\omega^2 = 32.08$ $\omega^2 = 37.54$ $\omega^2 = 37.95$

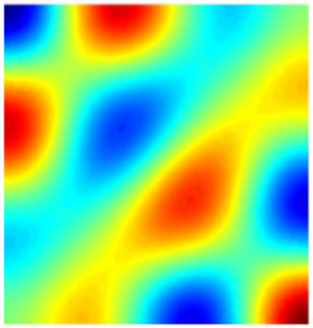 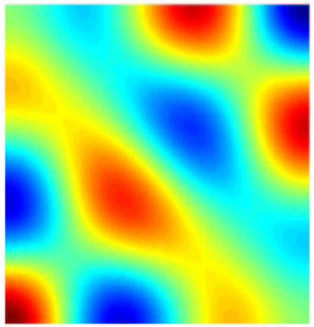 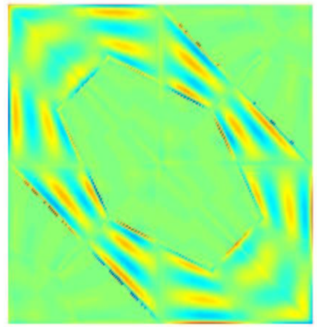 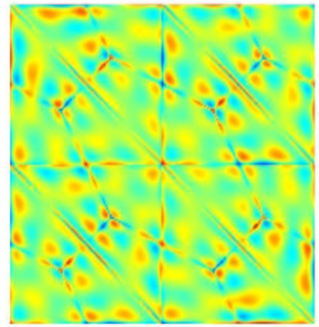

$\omega^2 = 37.98$ $\omega^2 = 38.00$ $\omega^2 = 38.03$ $\omega^2 = 38.03$

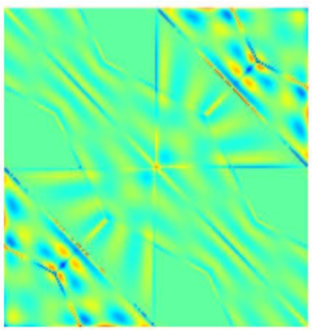 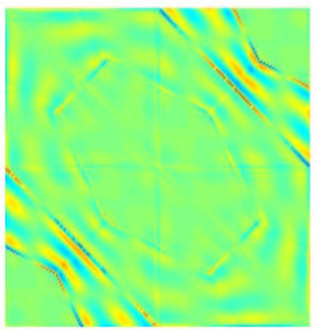 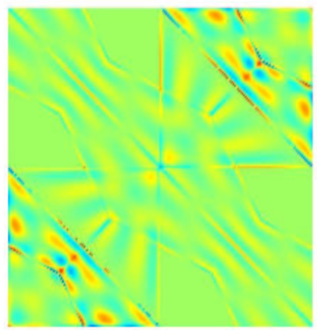 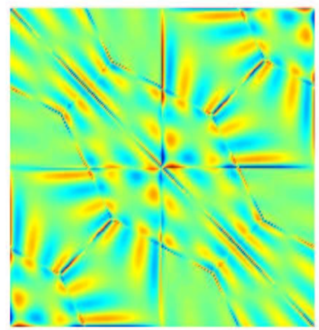

Eigenmodes with the second family

$\omega^2 = 37.98$

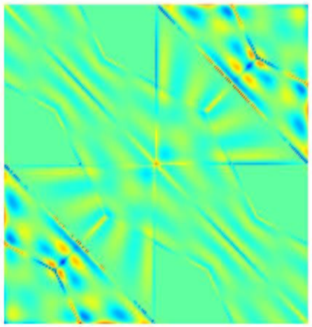

$\omega^2 = 38.00$

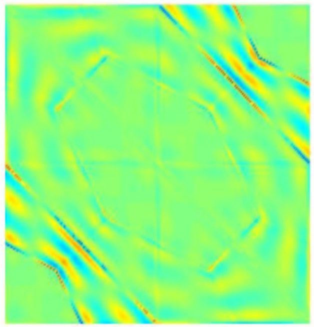

$\omega^2 = 38.03$

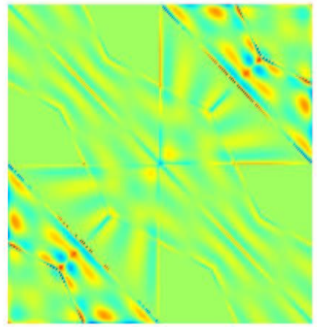

$\omega^2 = 38.03$

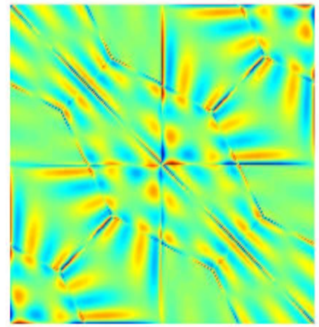

$\omega^2 = 38.04$

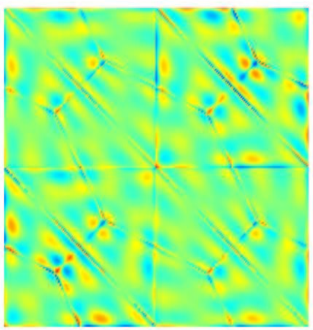

$\omega^2 = 38.05$

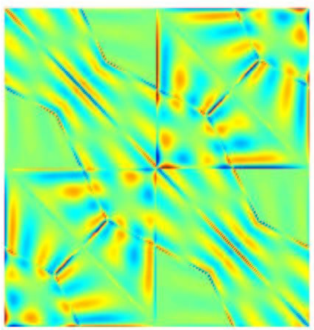

$\omega^2 = 38.07$

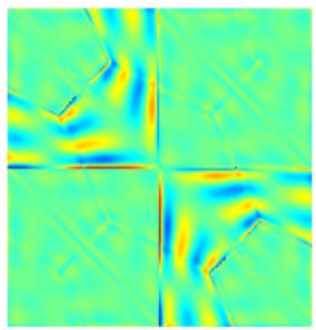

$\omega^2 = 38.20$

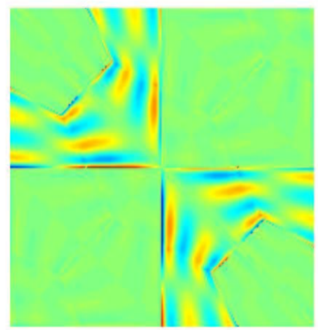

Eigenmodes with the second family

$\omega^2 = 38.04$ $\omega^2 = 38.05$ $\omega^2 = 38.07$ $\omega^2 = 38.20$

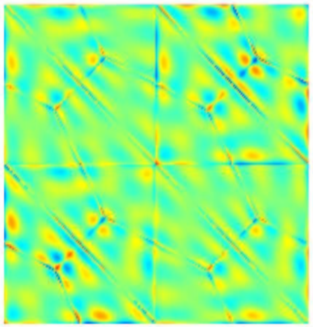
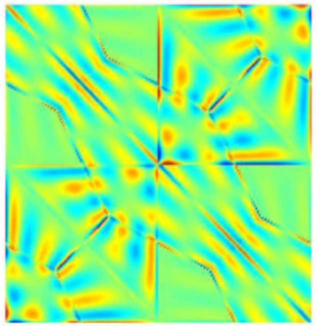
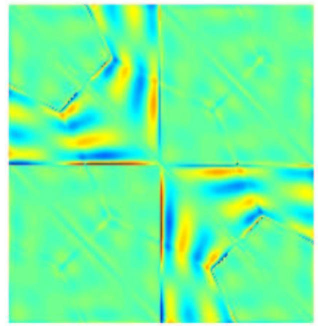
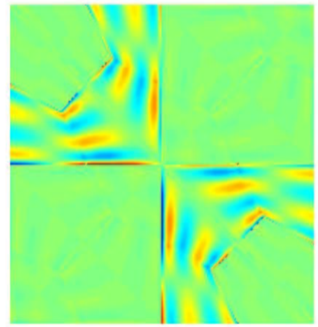

$\omega^2 = 39.48$ $\omega^2 = 39.48$ $\omega^2 = 41.95$ $\omega^2 = 41.95$

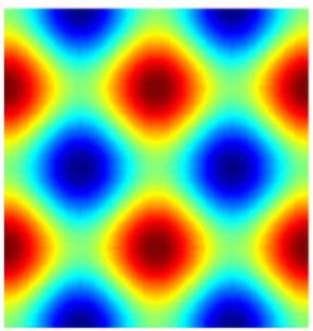
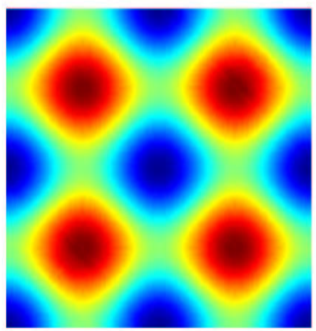
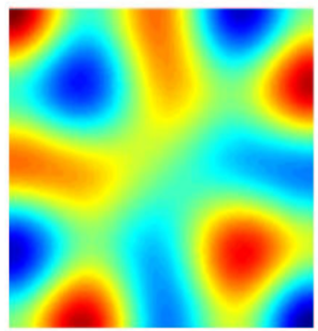
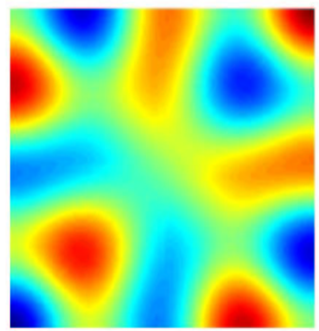

Eigenvalues with the second family

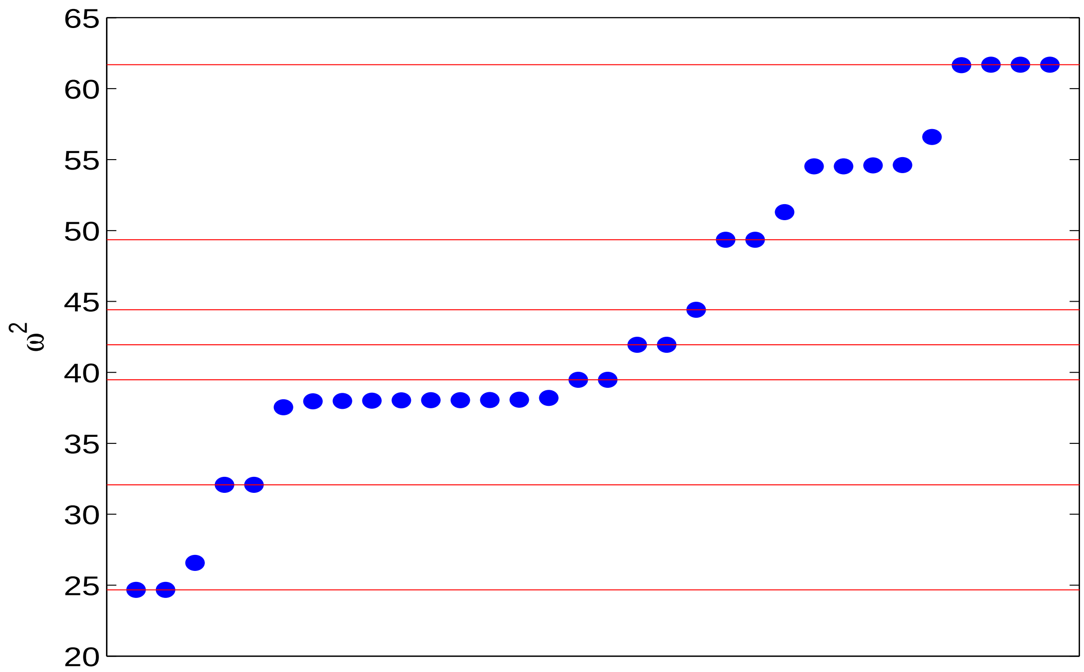

Eigenvalues with a non-regular mesh.

Analytical eigenvalues are symbolized by red lines.

Eigenvalues with the second family

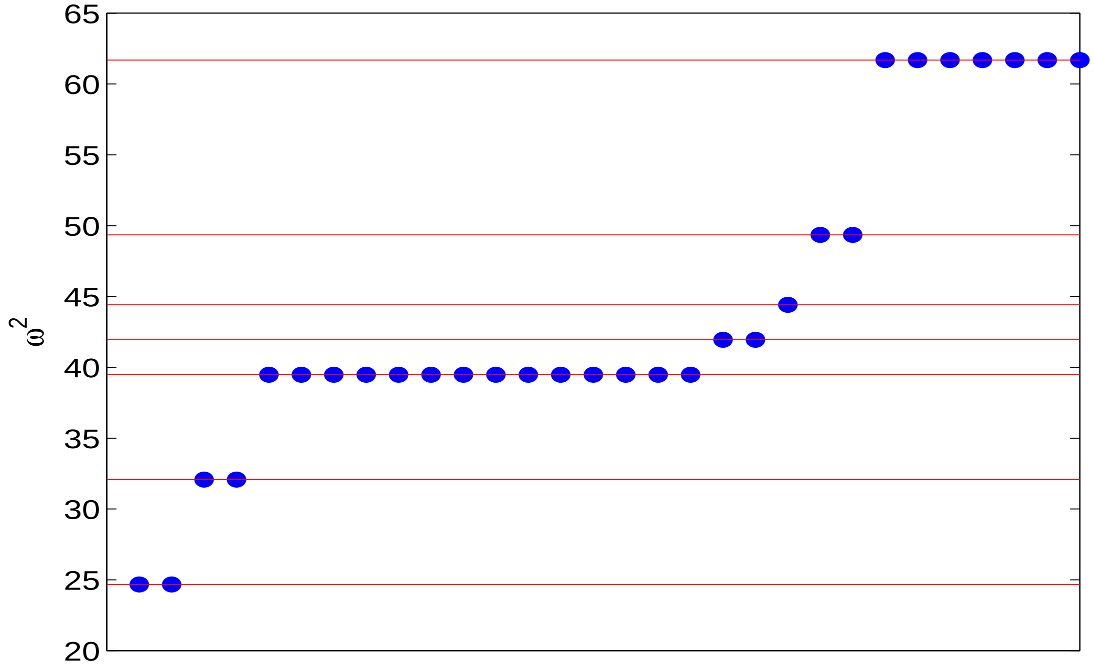

Eigenvalues with a regular mesh (incorrect multiplicity)

Eigenvalues with the second family

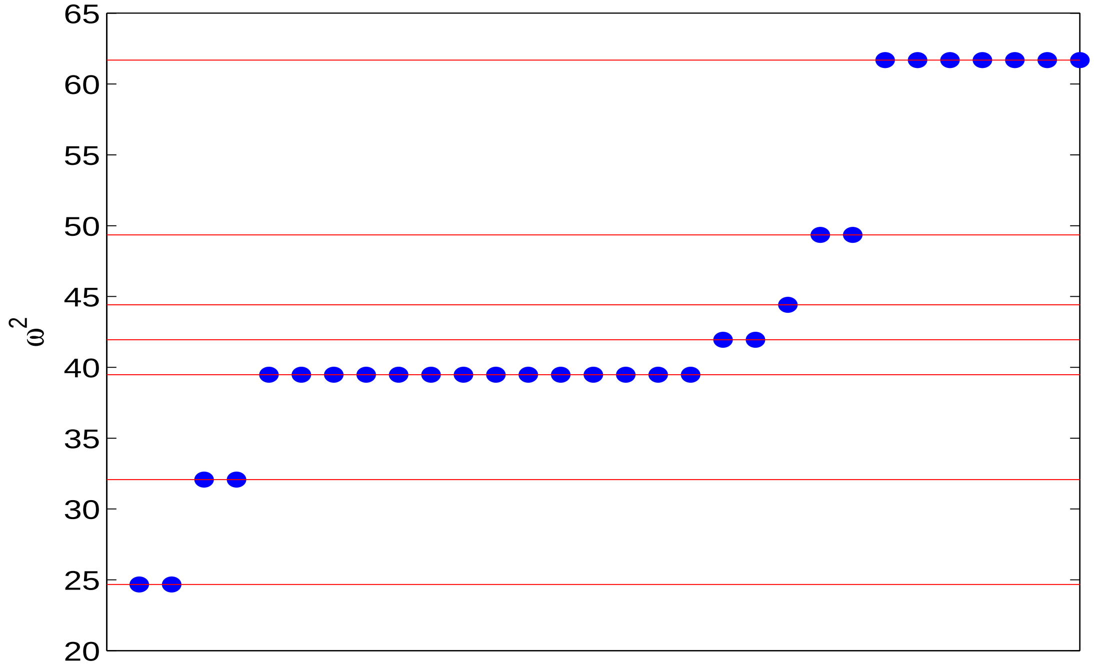

Eigenvalues with a regular mesh (incorrect multiplicity)

- Spurious eigenvalues and modes are dependent of the mesh.
- Nedelec's second family is NOT spectrally correct on quadrilaterals
- Nedelec's second family seems spectrally correct on triangles.

Consequency of spurious modes

Gaussian source at the center of the square, and $\omega^2 = 38.00$

Consequency of spurious modes

Gaussian source at the center of the square, and $\omega^2 = 38.00$

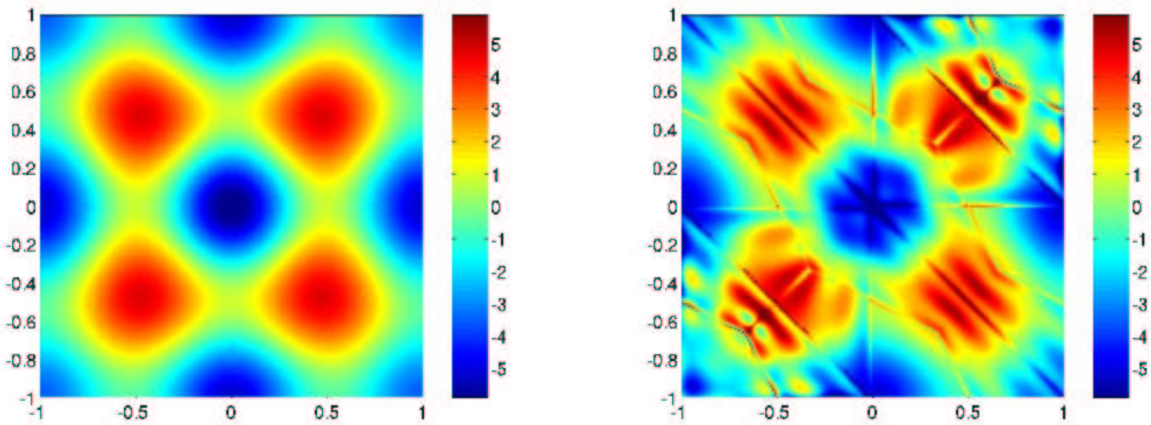

Solution with Q5 for the first (left) and second family (right)

Discontinuous Galerkin variational formulation

System in $\vec{E}$ and H

$$
\begin{aligned}
-k^2 \int_{K_i} \epsilon_r \vec{E} \cdot \vec{\varphi} \quad &- \int_{K_i} H \, \nabla \times \vec{\varphi} \quad - \int_{\partial K_i} \{H\} \, \vec{\varphi} \times \vec{\nu} \quad &= \quad 0 \\
\int_{K_i} \mu_r H \, \psi \quad &+ \int_{K_i} \nabla \times \vec{E} \, \psi \quad + \frac{1}{2} \int_{\partial K_i} [\vec{E}] \times \vec{\nu} \, \psi \quad &= \quad 0
\end{aligned}
\tag{5}
$$

Discontinuous Galerkin variational formulation

System in $\vec{E}$ and H

$$-k^2 \int_{K_i} \epsilon_r \vec{E} \cdot \vec{\varphi} \quad - \int_{K_i} H \, \nabla \times \vec{\varphi} \quad - \int_{\partial K_i} \{H\} \, \vec{\varphi} \times \vec{\nu} \quad = \quad 0$$

$$\int_{K_i} \mu_r H \, \psi \qquad + \int_{K_i} \nabla \times \vec{E} \, \psi \quad + \frac{1}{2} \int_{\partial K_i} [\vec{E}] \times \vec{\nu} \, \psi \quad = \quad 0$$

(5)

Let us remind that

$$\begin{aligned} \{H\} &= \tfrac{1}{2}(H_i + H_j) \\ [\,\vec{E}] &= (\vec{E}_i - \vec{E}_j) \end{aligned} \qquad (5)$$

Eigenvectors with DG on quadrilaterals

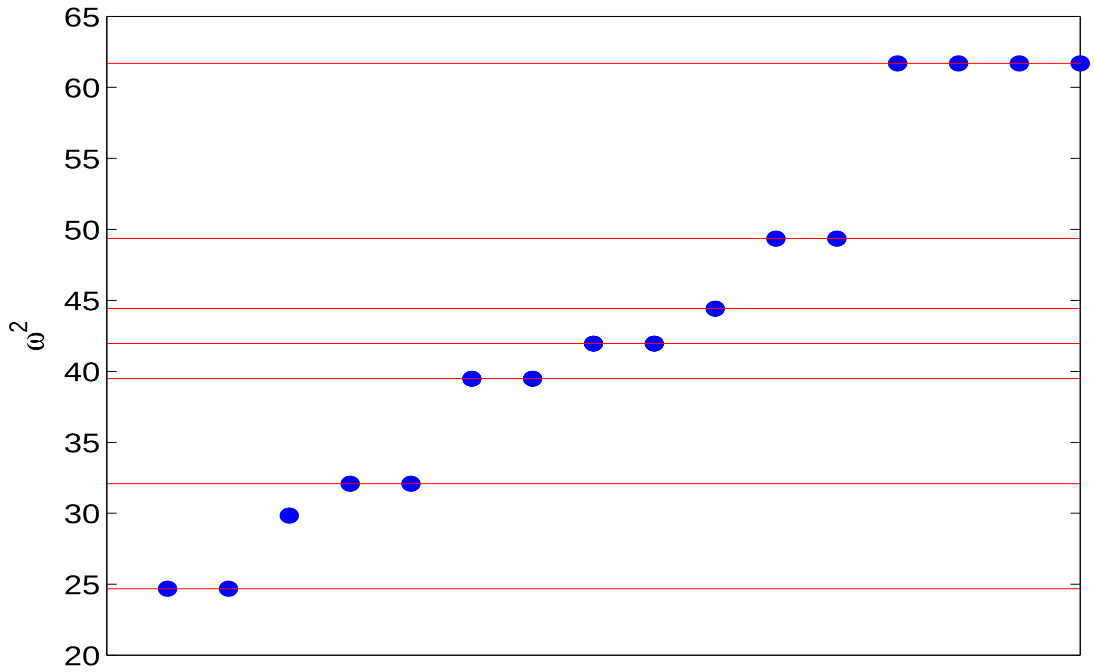

Eigenvalues, only one spurious mode.

Eigenvectors with DG on quadrilaterals

$\omega^2 = 26.92$ $\omega^2 = 32.08$ $\omega^2 = 32.08$ $\omega^2 = 39.48$

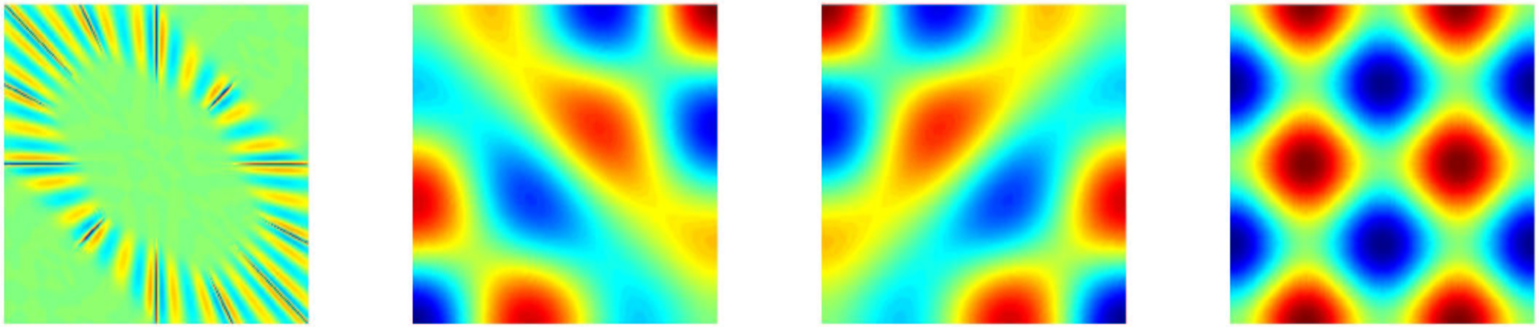

Eigenvectors with DG on quadrilaterals

$\omega^2 = 26.92$

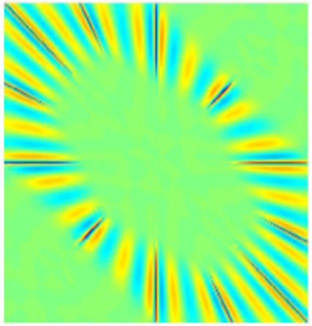

$\omega^2 = 32.08$

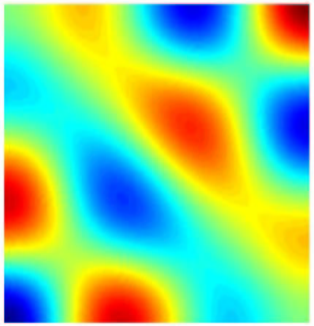

$\omega^2 = 32.08$

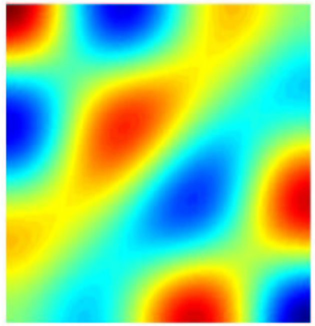

$\omega^2 = 39.48$

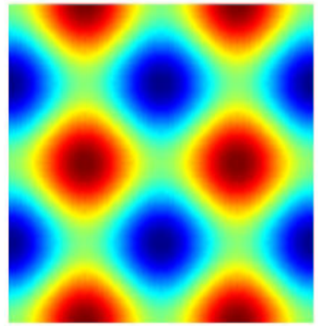

$\omega^2 = 39.48$

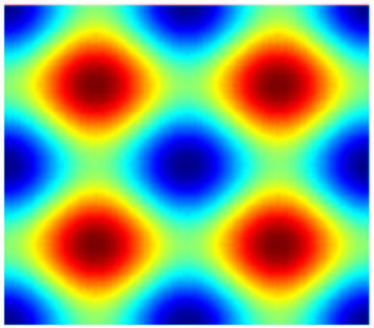

$\omega^2 = 41.95$

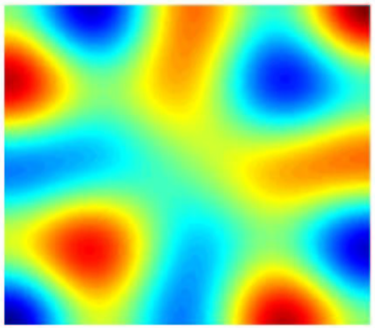

$\omega^2 = 41.95$

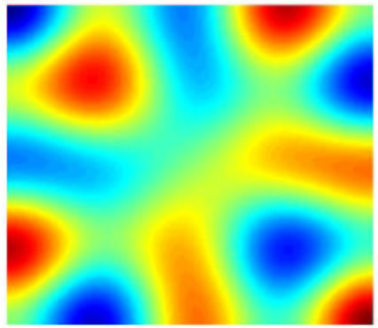

- DG method is NOT spectrally correct on quadrilaterals.

Study of the scattering of a perfectly conducting disk

Scattering by a disk of diameter 20 wavelengths

Study of the scattering of a perfectly conducting disk

Scattering by a disk of diameter 20 wavelengths

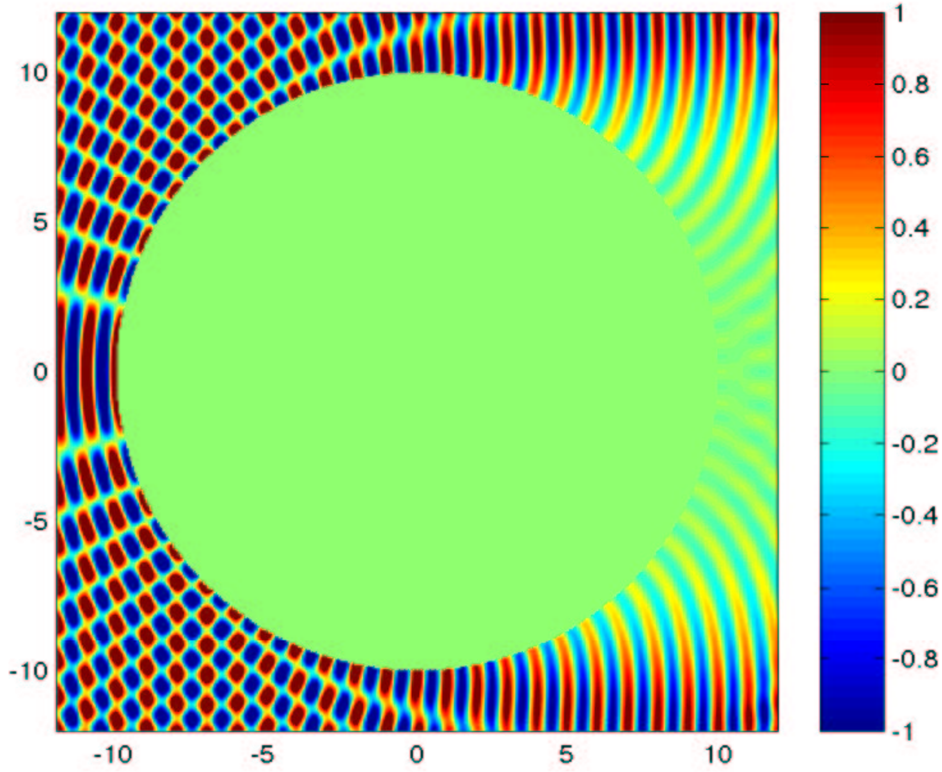

Study of the scattering of a perfectly conducting disk

Scattering by a disk of diameter 20 wavelengths

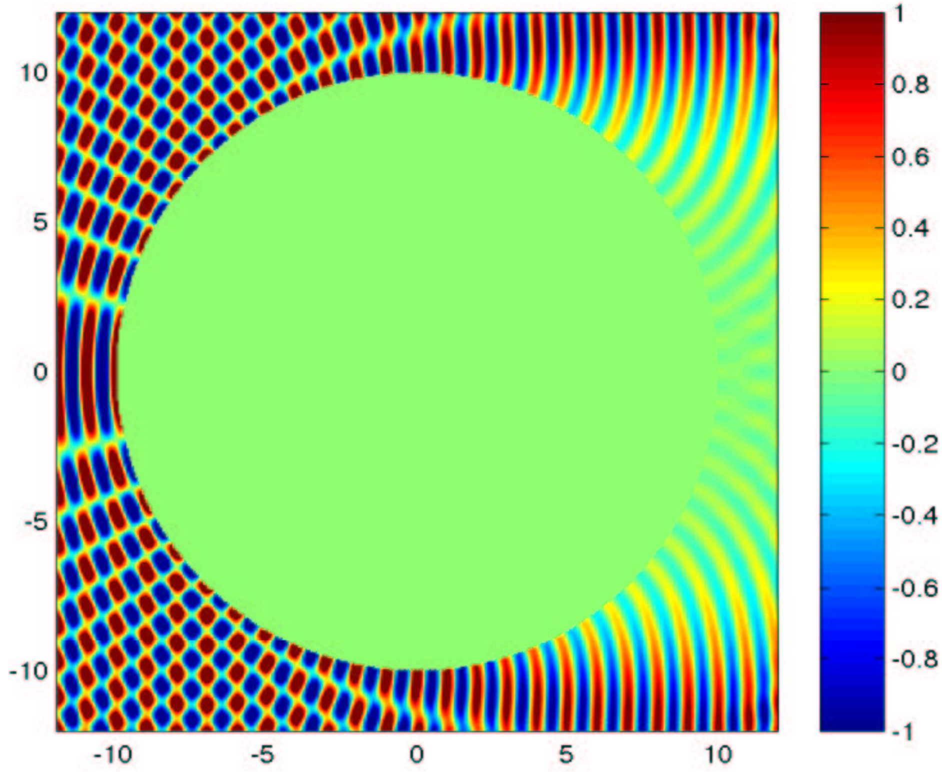

- Use of a transparency condition

Study of the scattering of a perfectly conducting disk

Scattering by a disk of diameter 20 wavelengths

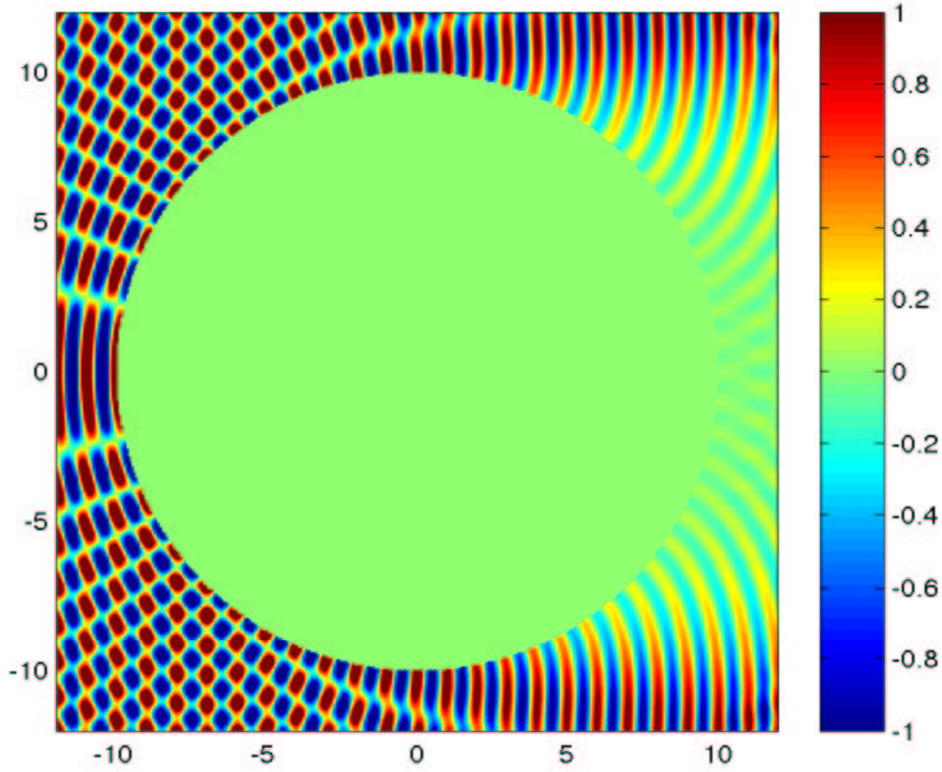

- Use of a transparency condition
- Use of curved elements

Comparison with finite edge elements

$H(\text{curl}, \Omega)$ error according the mesh step

Comparison with finite edge elements

$H(\text{curl}, \Omega)$ error according the mesh step

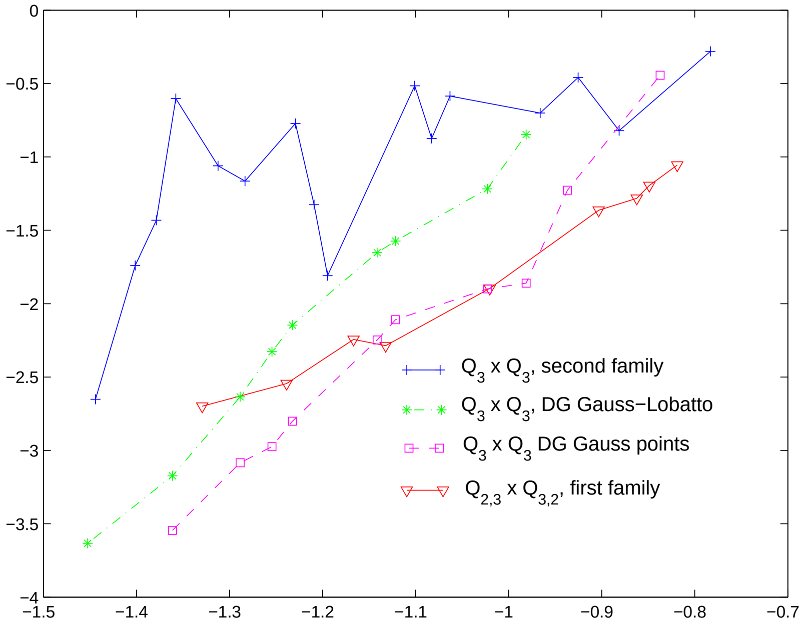

Comparison with finite edge elements

$H(\text{curl}, \Omega)$ error according the mesh step

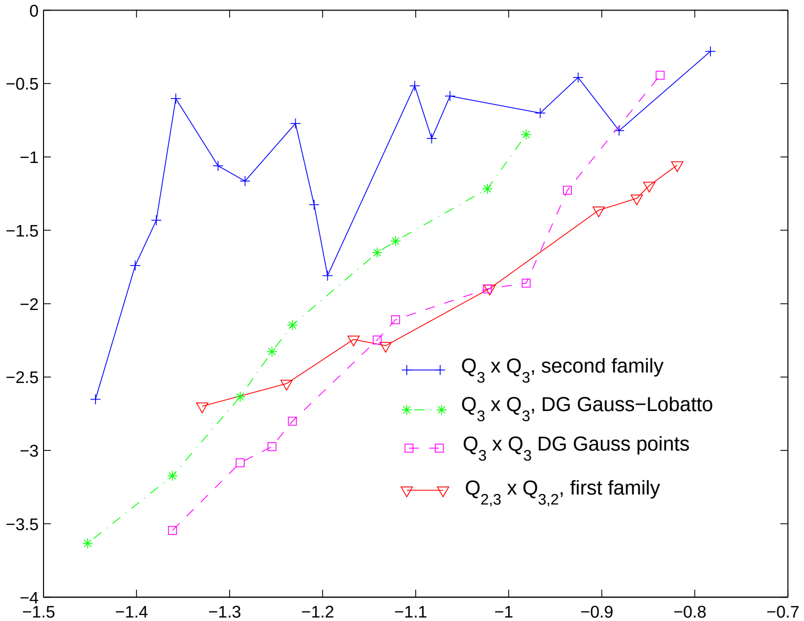

- Erratic convergence of second family

Comparison with finite edge elements

$H(\text{curl}, \Omega)$ error according the mesh step

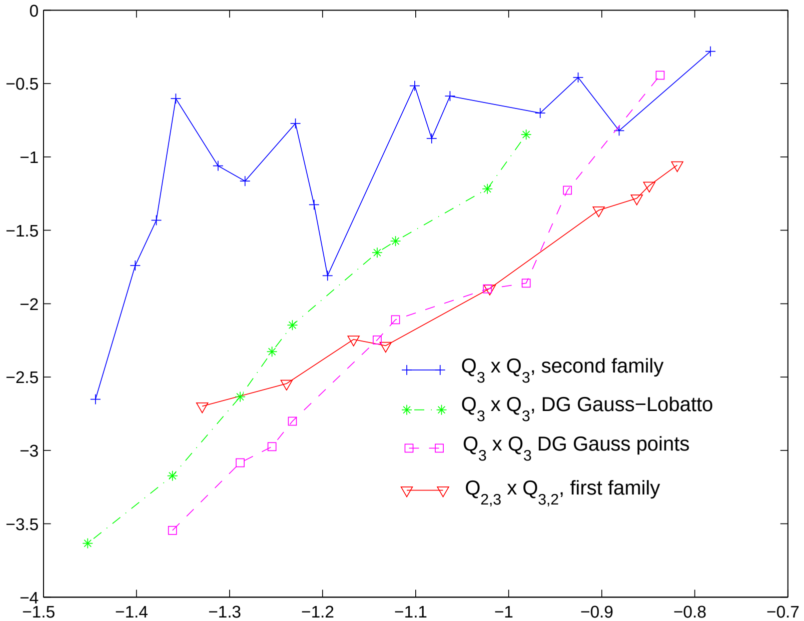

- Erratic convergence of second family
- Use of Gauss points for DG method gives better accuracy

Comparison with finite edge elements

$H(\text{curl}, \Omega)$ error according the mesh step

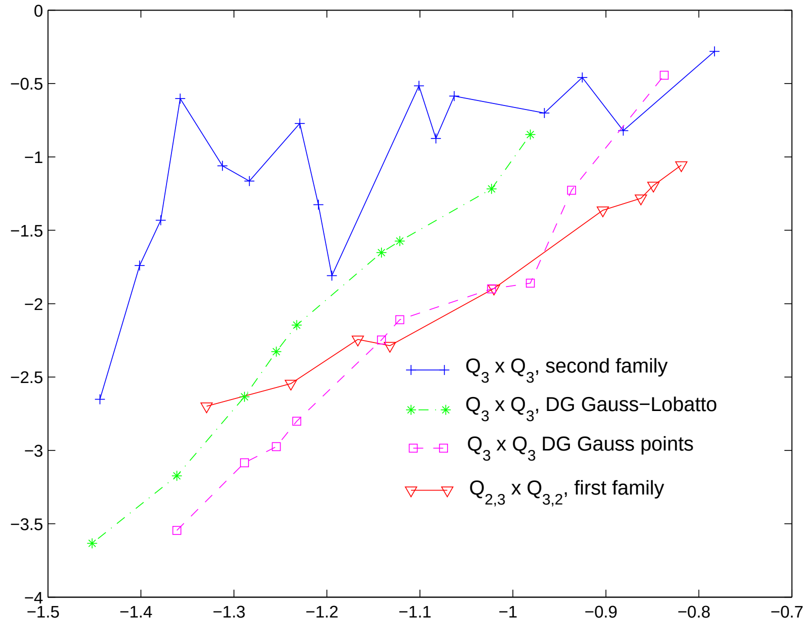

- Erratic convergence of second family
- Use of Gauss points for DG method gives better accuracy
- Order 3 of convergence for first family, order 4 for DG method

Scattering of a diedron-disk

Let us consider a diedron-disk coated by a dielectric
$(\varepsilon \;=\; 15 + 1.8i \qquad \mu \;=\; 1.7 + 1.7i)$

Scattering of a diedron-disk

Let us consider a diedron-disk coated by a dielectric
($\varepsilon = 15 + 1.8i \qquad \mu = 1.7 + 1.7i$)

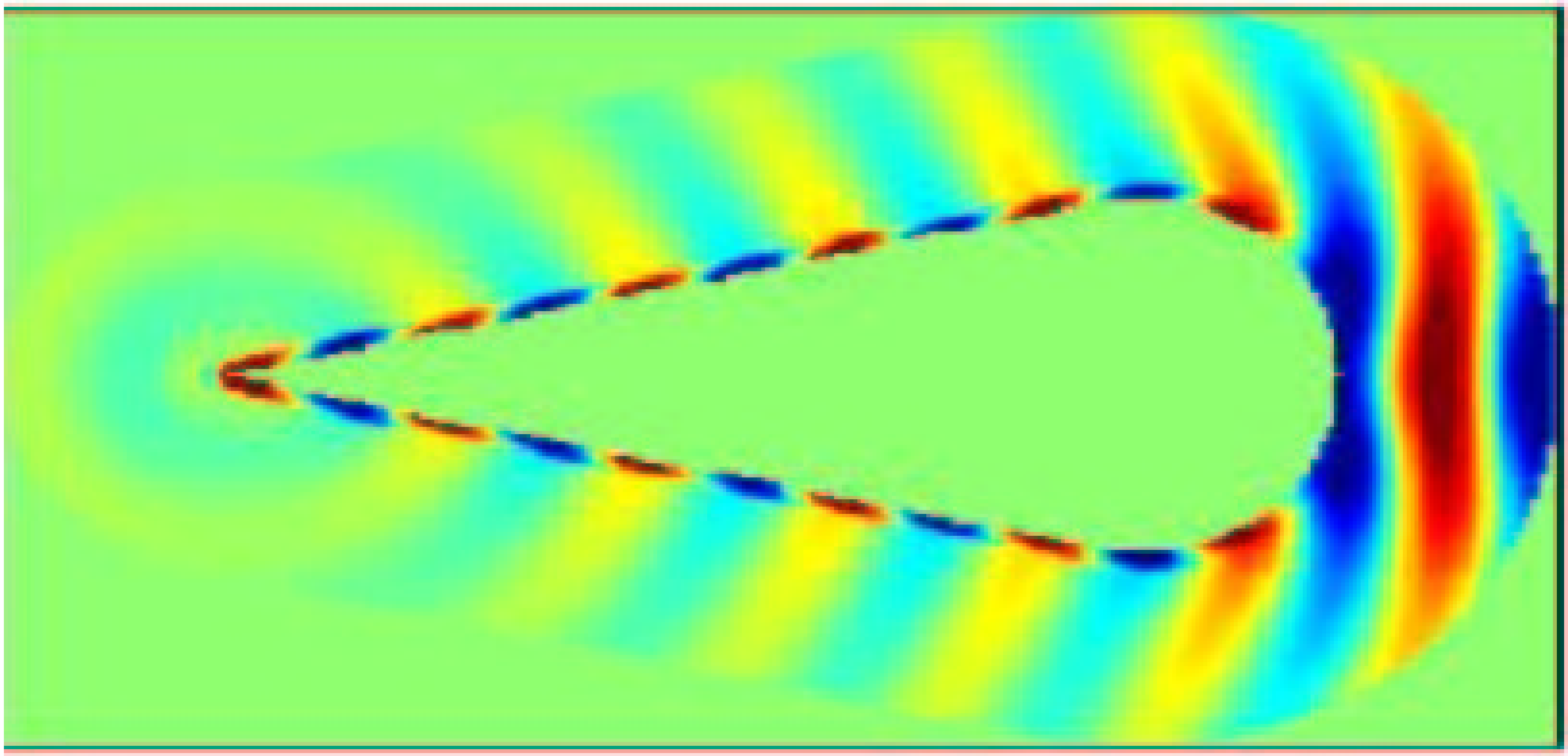

Diffracted field

Scattering of a diedron-disk

Let us consider a diedron-disk coated by a dielectric

$(\varepsilon = 15 + 1.8i \qquad \mu = 1.7 + 1.7i)$

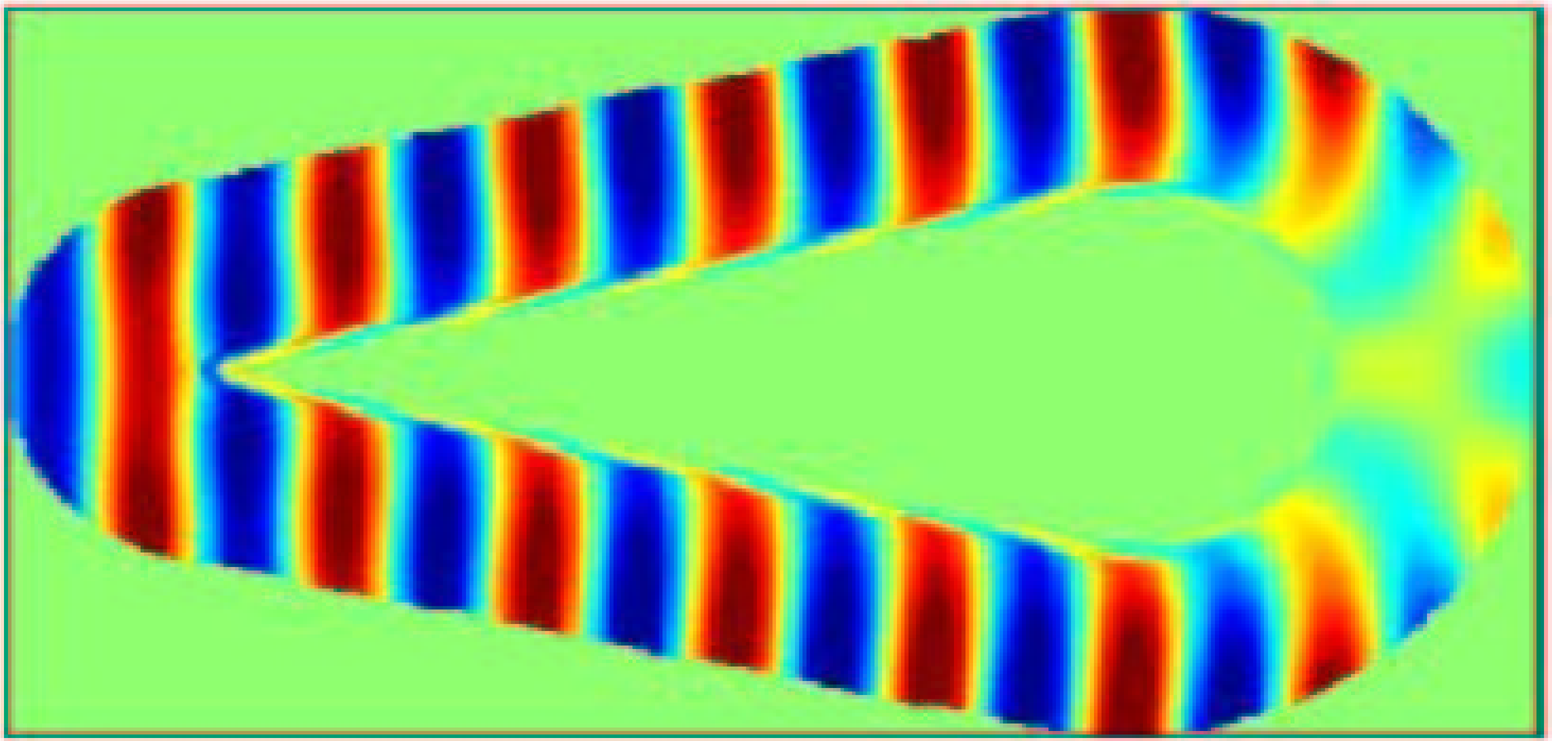

Total field

Scattering of a diedron-disk

Let us consider a diedron-disk coated by a dielectric
$(\varepsilon = 15 + 1.8i \qquad \mu = 1.7 + 1.7i)$

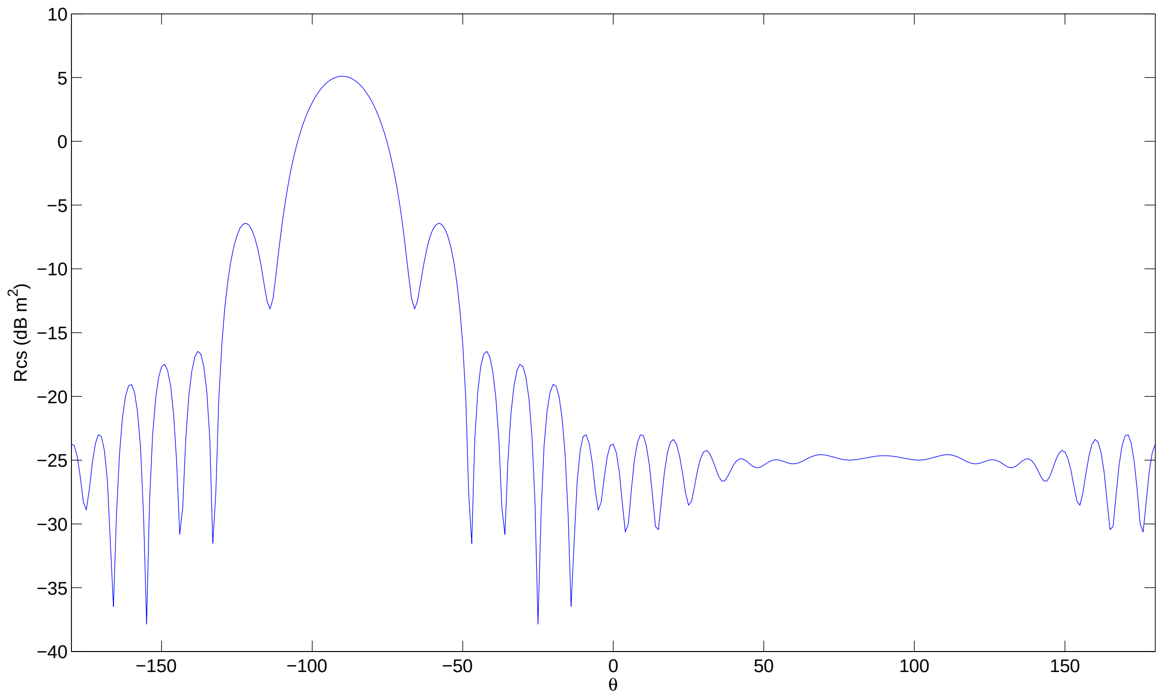

Radar Cross Section

Radar Cross Section

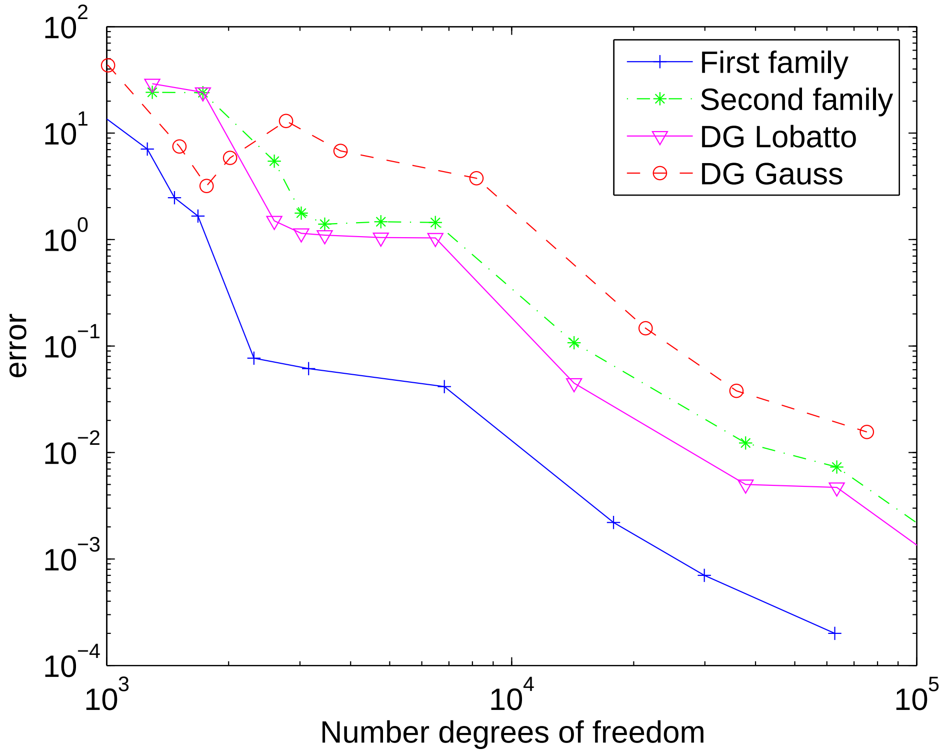

L^∞ error on the rcs according to the number of degrees of freedom (Q5).

Radar Cross Section

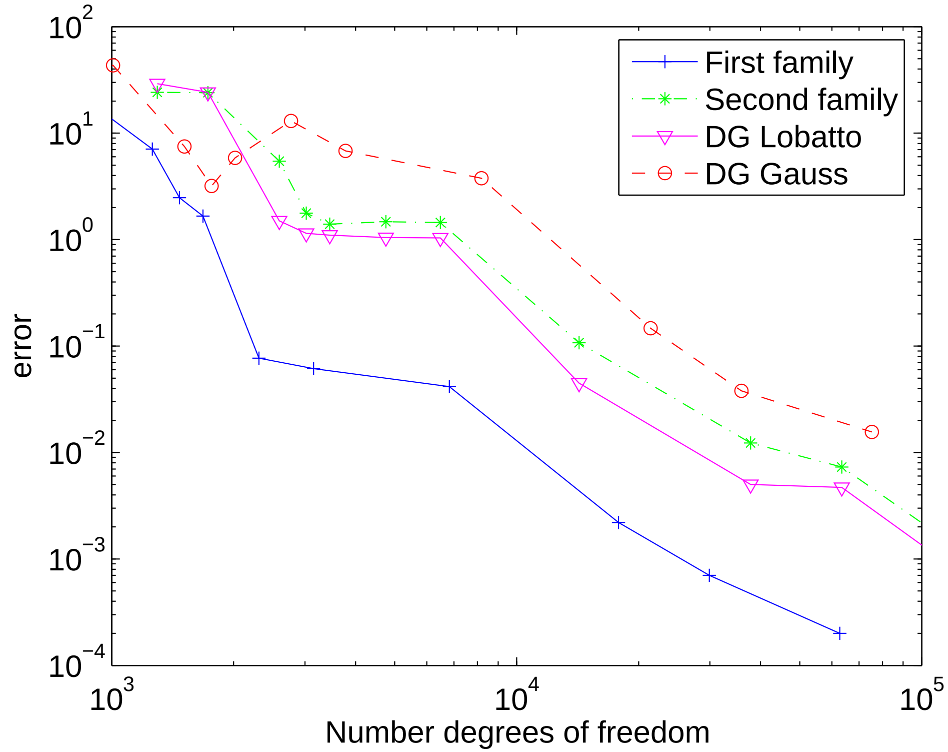

L^{∞} error on the rcs according to the number of degrees of freedom (Q5).

- First family on quadrilaterals is the most efficient
- No irregular convergence for the second family (use of a quasi-regular mesh)

Direct solver

Error level of 0.1dB

Direct solver

Error level of 0.1dB

Finite element	Number of dof	Memory used to factorize
First Family	$2\,300$	$3\,Mo$
Second Family	$21\,420$	$35\,Mo$
DG Lobatto	$14\,250$	$15\,Mo$

Direct solver

Error level of 0.1dB

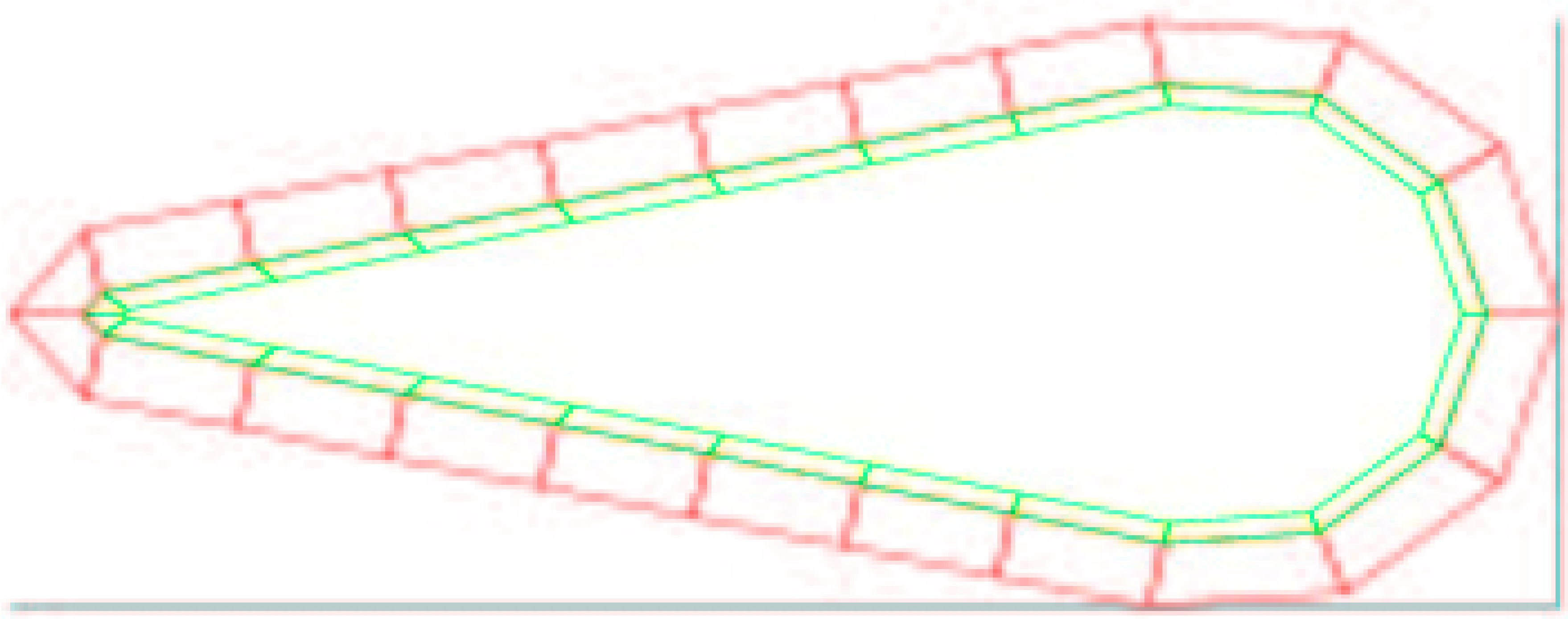

Mesh used for the first family

Direct solver

Error level of 0.1dB

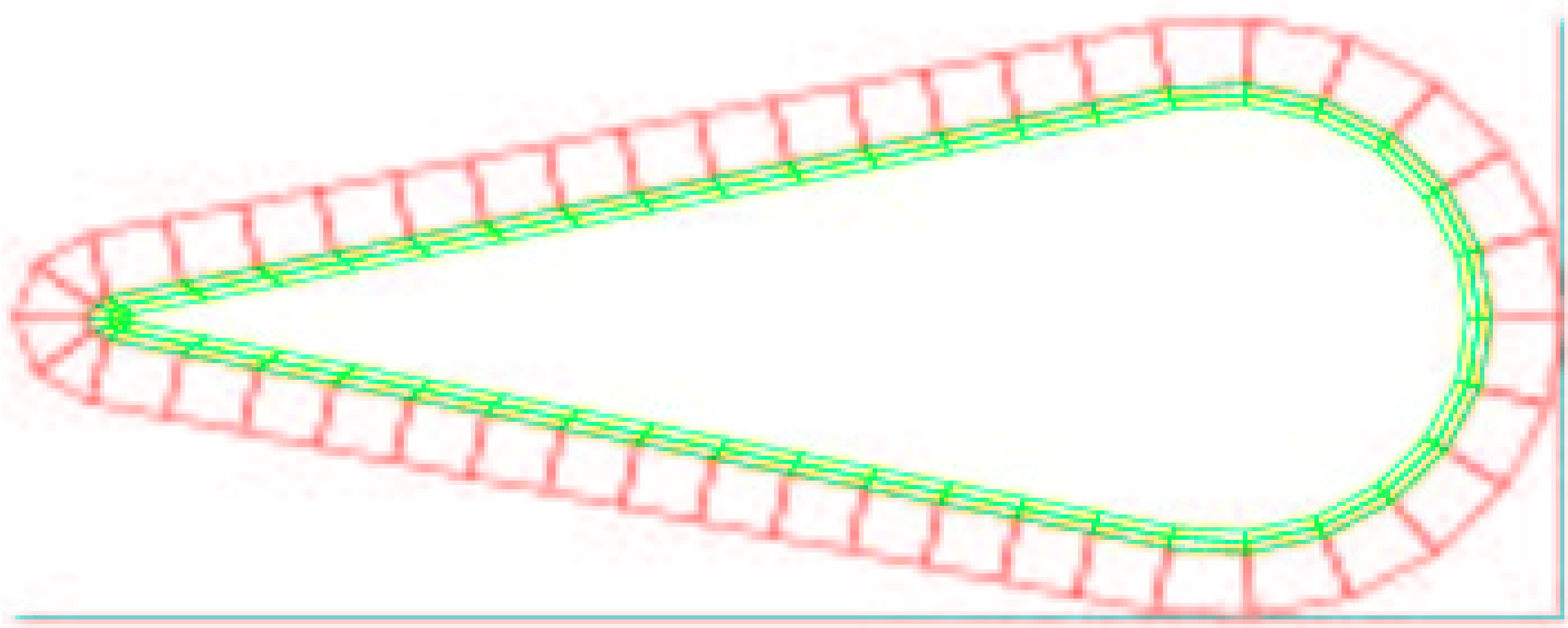

Mesh used for Discontinuous Galerkin method

Iterative solver

COCG (conjugate gradient for complex symmetric matrices) without preconditioning ($\varepsilon = 1e-6$)

Finite element	Number of iterations	Time
First Family	$4\,100$	$7\,s$
Second Family	$> 100\,000$	$-$
DG Lobatto	$> 100\,000$	$-$

Direct solver

Non-overlapping Schwarz method

Direct solver

Non-overlapping Schwarz method

Decomposition in subdomains $\Omega = \bigcup_{i=1}^{N_s} \Omega_i$

Direct solver

Non-overlapping Schwarz method

Decomposition in subdomains $\Omega = \bigcup_{i=1}^{N_s} \Omega_i$

$$M^{-1} = \sum_{i=1}^{N_s} P_i \, A_i^{-1} \, P_i^t$$

Direct solver

Non-overlapping Schwarz method

Decomposition in subdomains $\Omega = \bigcup_{i=1}^{N_s} \Omega_i$

$$M^{-1} = \sum_{i=1}^{N_s} P_i \, A_i^{-1} \, P_i^t$$

P_i, projection operator from Ω_i to Ω

A_i finite element matrix of Ω_i

Direct solver

Non-overlapping Schwarz method

Decomposition in subdomains $\Omega = \bigcup_{i=1}^{N_s} \Omega_i$

$$M^{-1} = \sum_{i=1}^{N_s} P_i \, A_i^{-1} \, P_i^t$$

P_i, projection operator from Ω_i to Ω

A_i finite element matrix of Ω_i

Factorization of matrices A_i with a direct solver (MUMPS)

Iterative solver with preconditioner

With 8 subdomains, we obtain :

Finite element	Number of iterations	Time
First Family	148	$1\,s$
Second Family	$3\,200$	$182\,s$
DG Lobatto	37	$1\,s$

Scattering by a sphere

Use of first family on hexahedrals, with Silver-Muller condition and curved elements.

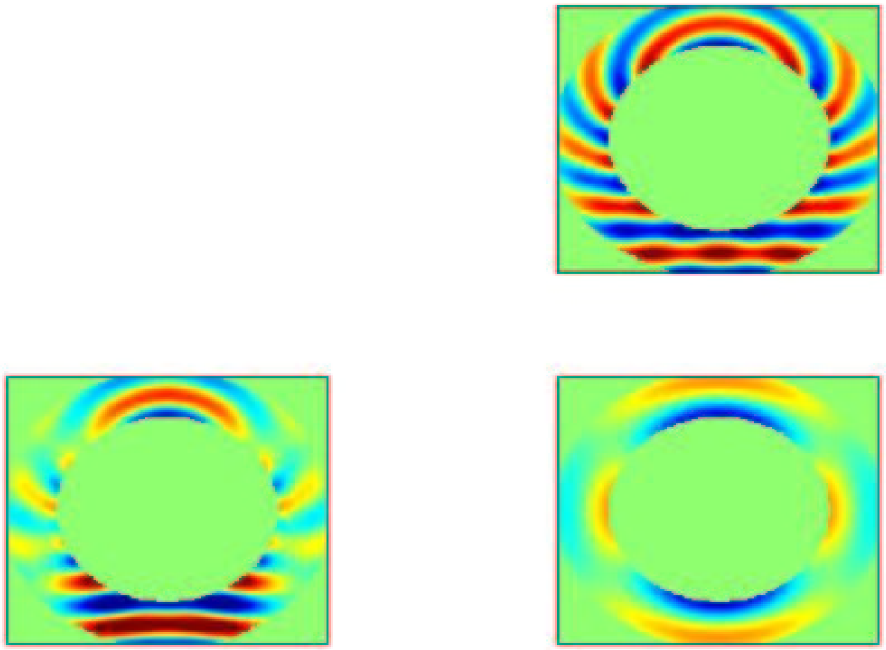

Diffracted field (real part of E_x) on three planes

Scattering by a sphere

Use of first family on hexahedrals, with Silver-Muller condition and curved elements.

Results for COCG without preconditioning ($\varepsilon = 1e - 6$)

Order	Number dof	Memory used	Number iterations	Time
5	$120\,000$	$30\,Mo$	$6\,800$	$940\,s$

Use of a specific matrix-vector product in order to have a low storage

(Gain of time too).